Investigation of the field-induced ferromagnetic phase transition in spin-polarized neutron matter: A lowest order constrained variational approach

G. H. Bordbar,[1,2,*] Z. Rezaei,[1] and Afshin Montakhab[1]
[1]*Department of Physics, Shiraz University, Shiraz 71454, Iran*
[2]*Research Institute for Astronomy and Astrophysics of Maragha, P.O. Box 55134-441, Maragha 55177-36698, Iran*
(Received 23 August 2010; revised manuscript received 28 September 2010; published 13 April 2011)

In this article, the lowest order constrained variational method is used to investigate the magnetic properties of spin-polarized neutron matter in the presence of strong magnetic field at zero temperature employing the AV_{18} potential. Our results indicate that a ferromagnetic phase transition is induced by a strong magnetic field with strength greater than 10^{18} G, leading to a partial spin polarization of the neutron matter. It is also shown that the equation of state of neutron matter in the presence of a magnetic field is stiffer than in the absence of a magnetic field.

DOI: 10.1103/PhysRevC.83.044310 PACS number(s): 21.65.−f, 26.60.−c, 64.70.−p

I. INTRODUCTION

The magnetic field of neutron stars most probably originates from the compression of magnetic flux inherited from the progenitor star [1]. Using this point of view, Woltjer predicted a magnetic field strength of order 10^{15} G for neutron stars [2]. The field can be distorted or amplified by some mixture of convection, differential rotation, and magnetic instabilities [3,4]. The relative importance of these ingredients depends on the initial field strength and the rotation rate of the star. For both convection and differential rotation, the field and its supporting currents are not likely to be confined to the solid crust of the star but instead distributed in most of the stellar interior, which is mostly a fluid mixture of neutrons, protons, electrons, and other more exotic particles [1]. Thompson *et al.* [5] argued that newborn neutron stars probably combine vigorous convection and differential rotation, making it likely that a dynamo process might operate in them. They expected fields up to 10^{15}–10^{16} G in neutron stars with few-millisecond initial periods. However, according to the scalar virial theorem which is based on Newtonian gravity, the magnetic field strength is allowed by values up to 10^{18} G in the interior of a magnetar [6]. However, general relativity predicts the allowed maximum value of a neutron star magnetic field to be about 10^{18}–10^{20} G [7]. By comparing with the observational data, Yuan *et al.* [8] obtained a magnetic field strength of order 10^{19} G for neutron stars.

The strong magnetic field could have an important influence on the interior matter of a neutron star. Many studies have dealt with the magnetic properties and the equation of state of neutron star matter [9–20] and quark star matter [21–26] in the presence of strong magnetic fields. Some authors have considered the influence of strong magnetic fields on neutron star matter within the mean-field approximation [9,12]. Yuan *et al.* [9], using the nonlinear σ-ω model, showed that the equation of state of neutron star matter becomes softer as the magnetic field increases. Also, Broderick *et al.* [10], employing a field theoretical approach in which baryons interact via the exchange of σ-ω-ρ mesons, observed that the softening of the equation of state caused by Landau quantization is overwhelmed by stiffening due to the incorporation of the anomalous magnetic moments of the nucleons. It was shown that the strong magnetic field shifts the β equilibrium and increases the proton fraction in neutron star matter [10–12]. Yue *et al.* [13] studied neutron star matter in the presence of a strong magnetic field using the quark-meson coupling model. Their results indicate that the Landau quantization of charged particles causes a softening in the equation of state, whereas the inclusion of nucleon anomalous magnetic moments leads to a stiffer equation of state. The effects of the magnetic field on neutron star structure, through its influence on the metric, was studied by Cardall *et al.* [27]. Their results show that the maximum mass, in a static configuration for a neutron star with magnetic field, is larger than the maximum mass obtained by uniform rotation. Through a field theoretical approach (at the mean-field level) in which the baryons interact via the exchange of σ-ω-ρ mesons, Broderick *et al.* [14] considered the effects of a magnetic field on the equation of state of dense baryonic matter in which hyperons are present. They found that, when the hyperons appear, the pressure becomes smaller than in the case of pure nucleonic matter for all fields. Within a relativistic Hartree approach in the linear σ-ω-ρ model, the effects of a magnetic field on cold symmetric nuclear matter and the nuclear matter in β equilibrium were investigated by Chakrabarty *et al.* [15]. Their results suggest that the neutron star mass is practically insensitive to the effects of the magnetic fields, whereas the radius decreases in intense fields.

In some studies, the neutron star matter was approximated by pure neutron matter. Isayev *et al.* [16] considered neutron matter in a strong magnetic field with the Skyrme effective interaction and analyzed the resultant self-consistent equations. They found that the thermodynamically stable branch extends from very low densities to the high-density region where the spin-polarization parameter is saturated, and neutrons become totally spin polarized. Perez-Garcia *et al.* [18–20] studied the effects of a strong magnetic field on pure neutron matter with effective nuclear forces within the framework of the nonrelativistic Hartree-Fock approximation. They showed that in the Skyrme model there is a ferromagnetic phase transition at $\rho \sim 4\rho_0$ (where $\rho_0 = 0.16$ fm^{-3} is the nuclear saturation density), whereas it is forbidden in the D1P

*Corresponding author: bordbar@physics.susc.ac.ir

model [18]. In addition to these findings, they found that the neutrino opacity of magnetized matter decreases compared to the nonmagnetized case for a magnetic field greater than 10^{17} G [19]. However, more realistically, for the problem of neutron star matter in the astrophysics context, it is necessary to consider the finite temperature [17,18,23,24] and finite proton fraction effects [9–15]. Isayev *et al.* [17] showed that the influence of finite temperatures on spin polarization remains moderate in the Skyrme model, at least up to temperatures relevant for protoneutron stars. It was also shown that for SLy4 effective interaction, even a small admixture of protons to neutron matter leads to a considerable shift of the critical density of the spin instability to lower values. For the SkI5 force, however, a small admixture of protons to neutron matter does not considerably change the critical density of the spin instability and increases its value [28].

In our previous works, we studied spin-polarized neutron matter [29], symmetric nuclear matter [30], asymmetric nuclear matter [31], and neutron star matter [31] at zero temperature using the lowest order constrained variational (LOCV) method with realistic strong interaction in the absence of a magnetic field. We also investigated the thermodynamic properties of spin-polarized neutron matter [32], symmetric nuclear matter [33], and asymmetric nuclear matter [34] at finite temperature with no magnetic field. In the above calculations, our results do not show any spontaneous ferromagnetic phase transition for these systems. In the present work, we study the magnetic properties of spin-polarized neutron matter at zero temperature in the presence of a strong magnetic field using the LOCV technique and employing AV_{18} potential.

II. LOCV FORMALISM FOR SPIN-POLARIZED NEUTRON MATTER

We consider pure homogeneous spin-polarized neutron matter composed of spin-up (+) and spin-down (−) neutrons. We denote the number densities of spin-up and spin-down neutrons by $\rho^{(+)}$ and $\rho^{(-)}$, respectively. We introduce the spin-polarization parameter (δ) by

$$\delta = \frac{\rho^{(+)} - \rho^{(-)}}{\rho}, \tag{1}$$

where $-1 \leqslant \delta \leqslant 1$, and $\rho = \rho^{(+)} + \rho^{(-)}$ is the total density of system.

To calculate the energy of this system, we use the LOCV method as follows. We consider a trial many-body wave function of the form

$$\psi = F\phi, \tag{2}$$

where ϕ is the uncorrelated ground-state wave function of N independent neutrons, and F is a proper N-body correlation function. Using the Jastrow approximation [35], F can be replaced by

$$F = S\prod_{i>j} f(ij), \tag{3}$$

where S is a symmetrizing operator. We consider a cluster expansion of the energy functional up to the two-body term,

$$E([f]) = \frac{1}{N}\frac{\langle\psi|H|\psi\rangle}{\langle\psi|\psi\rangle} = E_1 + E_2 \cdot \tag{4}$$

Now, we calculate the energy per particle up to the two-body term for two cases, in the absence and presence of the magnetic field, in two separate sections.

A. Energy calculation for spin-polarized neutron matter in the absence of a magnetic field

The one-body term E_1 for spin-polarized neutron matter in the absence of a magnetic field ($B = 0$) is given by

$$E_1^{(B=0)} = \sum_{i=+,-} \frac{3}{5}\frac{\hbar^2 k_F^{(i)^2}}{2m}\frac{\rho^{(i)}}{\rho}, \tag{5}$$

where $k_F^{(i)} = (6\pi^2\rho^{(i)})^{\frac{1}{3}}$ is the Fermi momentum of a neutron with spin projection i.

The two-body energy E_2 is

$$E_2^{(B=0)} = \frac{1}{2N}\sum_{ij}\langle ij|\nu(12)|ij - ji\rangle, \tag{6}$$

where

$$\nu(12) = -\frac{\hbar^2}{2m}\left[f(12),\left[\nabla_{12}^2, f(12)\right]\right] + f(12)V(12)f(12).$$

In the preceding equation, $f(12)$ and $V(12)$ are the two-body correlation function and the nuclear potential, respectively. In our calculations, we employ the AV_{18} two-body potential [36],

$$V(12) = \sum_{p=1}^{18} V^{(p)}(r_{12})O_{12}^{(p)}, \tag{7}$$

where

$$O_{12}^{(p=1,\ldots,18)} = 1, \sigma_1\cdot\sigma_2, \tau_1\cdot\tau_2, (\sigma_1\cdot\sigma_2)(\tau_1\cdot\tau_2), S_{12}, S_{12}(\tau_1\cdot\tau_2), \mathbf{L}\cdot\mathbf{S}, \mathbf{L}\cdot\mathbf{S}(\tau_1\cdot\tau_2), \mathbf{L}^2, \mathbf{L}^2(\sigma_1\cdot\sigma_2), \mathbf{L}^2(\tau_1\cdot\tau_2), \mathbf{L}^2(\sigma_1\cdot\sigma_2)(\tau_1\cdot\tau_2), (\mathbf{L}\cdot\mathbf{S})^2, (\mathbf{L}\cdot\mathbf{S})^2(\tau_1\cdot\tau_2), \mathbf{T}_{12}, (\sigma_1\cdot\sigma_2)\mathbf{T}_{12}, S_{12}\mathbf{T}_{12}, (\tau_{z1}+\tau_{z2}). \tag{8}$$

In the preceding equation,

$$S_{12} = [3(\sigma_1\cdot\hat{r})(\sigma_2\cdot\hat{r}) - \sigma_1\cdot\sigma_2]$$

is the tensor operator and

$$\mathbf{T}_{12} = [3(\tau_1\cdot\hat{r})(\tau_2\cdot\hat{r}) - \tau_1\cdot\tau_2]$$

is the isotensor operator. The above 18 components of the AV_{18} two-body potential are denoted by the labels c, σ, τ, $\sigma\tau$, t, $t\tau$, ls, $ls\tau$, $l2$, $l2\sigma$, $l2\tau$, $l2\sigma\tau$, $ls2$, $ls2\tau$, T, σT, tT, and τz, respectively [36]. In the LOCV formalism, the two-body correlation function $f(12)$ is considered as follows [37]:

$$f(12) = \sum_{k=1}^{3} f^{(k)}(r_{12})P_{12}^{(k)}, \tag{9}$$

where

$$P_{12}^{(k=1,\ldots,3)} = \left(\tfrac{1}{4} - \tfrac{1}{4}O_{12}^{(2)}\right),\ \left(\tfrac{1}{2} + \tfrac{1}{6}O_{12}^{(2)} + \tfrac{1}{6}O_{12}^{(5)}\right),\ \left(\tfrac{1}{4} + \tfrac{1}{12}O_{12}^{(2)} - \tfrac{1}{6}O_{12}^{(5)}\right). \tag{10}$$

The operators $O_{12}^{(2)}$ and $O_{12}^{(5)}$ are given in Eq. (8). Using the preceding two-body correlation function and potential, after doing some algebra, we find the following equation for the two-body energy:

$$\begin{aligned}
E_2^{(B=0)} = {} & \frac{2}{\pi^4\rho}\left(\frac{\hbar^2}{2m}\right)\sum_{JLSS_z}\frac{(2J+1)}{2(2S+1)}[1-(-1)^{L+S+1}]\left|\left\langle\frac{1}{2}\sigma_{z1}\frac{1}{2}\sigma_{z2}\right|SS_z\right\rangle\right|^2 \\
& \times\int dr\left\{\left[f_\alpha^{(1)'^2}a_\alpha^{(1)^2}(k_f r) + \frac{2m}{\hbar^2}\left(\{V_c - 3V_\sigma + V_\tau - 3V_{\sigma\tau} + 2(V_T - 3V_{\sigma T}) - 2V_{\tau z}\}a_\alpha^{(1)^2}(k_f r)\right.\right.\right. \\
& \left.\left.+[V_{l2} - 3V_{l2\sigma} + V_{l2\tau} - 3V_{l2\sigma\tau}]c_\alpha^{(1)^2}(k_f r)\right)(f_\alpha^{(1)})^2\right] + \sum_{k=2,3}\left[f_\alpha^{(k)'^2}a_\alpha^{(k)^2}(k_f r)\right. \\
& +\frac{2m}{\hbar^2}\left(\{V_c + V_\sigma + V_\tau + V_{\sigma\tau} + (-6k+14)(V_{t\tau} + V_t) - (k-1)(V_{ls\tau} + V_{ls})\right. \\
& +2[V_T + V_{\sigma T} + (-6k+14)V_{tT} - V_{\tau z}]\}a_\alpha^{(k)^2}(k_f r) + [V_{l2} + V_{l2\sigma} + V_{l2\tau} + V_{l2\sigma\tau}]c_\alpha^{(k)^2}(k_f r) \\
& \left.\left.+[V_{ls2} + V_{ls2\tau}]d_\alpha^{(k)^2}(k_f r)\right)f_\alpha^{(k)^2}\right] + \frac{2m}{\hbar^2}\{V_{ls} + V_{ls\tau} - 2(V_{l2} + V_{l2\sigma} + V_{l2\sigma\tau} + V_{l2\tau}) - 3(V_{ls2} + V_{ls2\tau})\}b_\alpha^2(k_f r)f_\alpha^{(2)}f_\alpha^{(3)} \\
& \left.+\frac{1}{r^2}\left(f_\alpha^{(2)} - f_\alpha^{(3)}\right)^2 b_\alpha^2(k_f r)\right\},
\end{aligned} \tag{11}$$

where $\alpha = \{J, L, S, S_z\}$ and the coefficients $a_\alpha^{(1)^2}$, etc., are defined as

$$a_\alpha^{(1)^2}(x) = x^2 I_{L,S_z}(x), \tag{12}$$

$$a_\alpha^{(2)^2}(x) = x^2\left[\beta I_{J-1,S_z}(x) + \gamma I_{J+1,S_z}(x)\right], \tag{13}$$

$$a_\alpha^{(3)^2}(x) = x^2\left[\gamma I_{J-1,S_z}(x) + \beta I_{J+1,S_z}(x)\right], \tag{14}$$

$$b_\alpha^{(2)}(x) = x^2\left[\beta_{23} I_{J-1,S_z}(x) - \beta_{23} I_{J+1,S_z}(x)\right], \tag{15}$$

$$c_\alpha^{(1)^2}(x) = x^2 \nu_1 I_{L,S_z}(x), \tag{16}$$

$$c_\alpha^{(2)^2}(x) = x^2\left[\eta_2 I_{J-1,S_z}(x) + \nu_2 I_{J+1,S_z}(x)\right], \tag{17}$$

$$c_\alpha^{(3)^2}(x) = x^2\left[\eta_3 I_{J-1,S_z}(x) + \nu_3 I_{J+1,S_z}(x)\right], \tag{18}$$

$$d_\alpha^{(2)^2}(x) = x^2\left[\xi_2 I_{J-1,S_z}(x) + \lambda_2 I_{J+1,S_z}(x)\right], \tag{19}$$

$$d_\alpha^{(3)^2}(x) = x^2\left[\xi_3 I_{J-1,S_z}(x) + \lambda_3 I_{J+1,S_z}(x)\right], \tag{20}$$

with

$$\beta = \frac{J+1}{2J+1},\quad \gamma = \frac{J}{2J+1},\quad \beta_{23} = \frac{2J(J+1)}{2J+1}, \tag{21}$$

$$\nu_1 = L(L+1),\quad \nu_2 = \frac{J^2(J+1)}{2J+1},$$

$$\nu_3 = \frac{J^3+2J^2+3J+2}{2J+1}, \tag{22}$$

$$\eta_2 = \frac{J(J^2+2J+1)}{2J+1},\quad \eta_3 = \frac{J(J^2+J+2)}{2J+1}, \tag{23}$$

$$\xi_2 = \frac{J^3+2J^2+2J+1}{2J+1},\quad \xi_3 = \frac{J(J^2+J+4)}{2J+1}, \tag{24}$$

$$\lambda_2 = \frac{J(J^2+J+1)}{2J+1},\quad \lambda_3 = \frac{J^3+2J^2+5J+4}{2J+1}, \tag{25}$$

and

$$I_{J,S_z}(x) = \int dq\, q^2 P_{S_z}(q) J_J^2(xq). \tag{26}$$

In the last equation, $J_J(x)$ is the Bessel function and $P_{S_z}(q)$ is defined as

$$\begin{aligned}
P_{S_z}(q) = {} & \tfrac{2}{3}\pi\left\{\left(k_F^{\sigma_{z1}}\right)^3 + \left(k_F^{\sigma_{z2}}\right)^3 - \tfrac{3}{2}\left[\left(k_F^{\sigma_{z1}}\right)^2 + \left(k_F^{\sigma_{z2}}\right)^2\right]q\right. \\
& \left. - \tfrac{3}{16}\left[\left(k_F^{\sigma_{z1}}\right)^2 - \left(k_F^{\sigma_{z2}}\right)^2\right]^2 q^{-1} + q^3\right\}
\end{aligned} \tag{27}$$

for $\frac{1}{2}|k_F^{\sigma_{z1}} - k_F^{\sigma_{z2}}| < q < \frac{1}{2}|k_F^{\sigma_{z1}} + k_F^{\sigma_{z2}}|$,

$$P_{S_z}(q) = \tfrac{4}{3}\pi \min\left(\left(k_F^{\sigma_{z1}}\right)^3, \left(k_F^{\sigma_{z2}}\right)^3\right) \tag{28}$$

for $q < \frac{1}{2}|k_F^{\sigma_{z1}} - k_F^{\sigma_{z2}}|$, and

$$P_{S_z}(q) = 0 \tag{29}$$

for $q > \frac{1}{2}|k_F^{\sigma_{z1}} + k_F^{\sigma_{z2}}|$, where σ_{z1} or $\sigma_{z2} = +1, -1$ for spin up and spin down, respectively.

B. Energy calculation of spin-polarized neutron matter in the presence of a magnetic field

Now we consider the case in which the spin-polarized neutron matter is under the influence of a strong magnetic field. Taking the uniform magnetic field along the z direction, $B = B\widehat{k}$, the spin-up and spin-down particles correspond to parallel and antiparallel spins with respect to the magnetic field. Therefore, the contribution of the magnetic energy of the neutron matter is

$$E_M = -M_z B, \tag{30}$$

where M_z is the magnetization of the neutron matter, which is given by

$$M_z = N\mu_n\delta. \tag{31}$$

In the preceding equation, $\mu_n = -1.9130427(5)$ is the neutron magnetic moment (in units of the nuclear magneton). Consequently, the energy per particle up to the two-body term in the presence of a magnetic field can be written as

$$E([f]) = E_1^{(B=0)} + E_2^{(B=0)} - \mu_n B\delta, \tag{32}$$

where $E_1^{(B=0)}$ and $E_2^{(B=0)}$ are given by Eqs. (5) and (11), respectively. It should be noted that in usual thermodynamic treatments the external magnetic field energy ($\frac{1}{8\pi}\int dV\, B^2$) is usually left out because it does not affect the thermodynamic properties of matter [38]. In fact, the magnetic field energy arises only from the magnetostatic energy in the absence of matter, but we are interested in the contribution of internal energy, which excludes the energy of magnetic field. Therefore, the magnetic field contribution, $E_{\text{mag}} = \frac{B^2}{8\pi}$, which is the *energy density* (or "magnetic pressure") of the magnetic field in the absence of matter, is usually omitted [16,38].

Now we minimize the two-body energy with respect to the variations in the function $f_\alpha^{(i)}$ subject to the normalization constraint [39],

$$\frac{1}{N}\sum_{ij}\langle ij|h_{S_z}^2 - f^2(12)|ij\rangle_a = 0, \tag{33}$$

where, in the case of spin-polarized neutron matter, the function $h_{S_z}(r)$ is defined as follows:

$$h_{S_z}(r) = \begin{cases} \left[1 - 9\left(\frac{J_J^2(k_F^{(i)}r)}{k_F^{(i)}r}\right)^2\right]^{-1/2}, & S_z = \pm 1, \\ 1, & S_z = 0. \end{cases} \tag{34}$$

From minimization of the two-body cluster energy, we get a set of coupled and uncoupled differential equations, which are the same as those presented in Ref. [39] but with the coefficients replaced by those indicated in Eqs. (12)–(20). By solving these differential equations, we can obtain correlation functions to compute the two-body energy.

III. RESULTS AND DISCUSSION

Our results for the energy per particle of spin-polarized neutron matter versus the spin-polarization parameter for different values of the magnetic field at $\rho = 0.2$ fm^{-3} are shown in Fig. 1. We found that for values of the magnetic field below 10^{18} G, the corresponding energies of different magnetic fields are nearly identical. This shows that the effect of a magnetic field below $B \sim 10^{18}$ G is nearly insignificant. From Fig. 1, we can see that the spin-polarization symmetry is broken when the magnetic field is present and a minimum appears at $-1 < \delta < 0$. By increasing the magnetic field strength from $B \sim 10^{18}$ to $B \sim 10^{19}$ G, the value of spin polarization corresponding to the minimum point approaches -1. We also see that, by increasing the magnetic field, the energy per particle at the minimum point (ground-state energy) decreases, leading to a more stable system. For each density, we found that, above a certain value of the magnetic field, the system reaches a saturation point and the minimum energy occurs at $\delta = -1$. For example, at $\rho = 0.2$ fm^{-3}, for $B \gtrsim 1.8 \times 10^{19}$ G, the minimum energy occurs at $\delta = -1$. However, this threshold value of the magnetic field increases when the density increases. In Fig. 2, we present the ground-state energy per particle of spin-polarized neutron matter as a function of the density for different values of the magnetic field. For each value of the magnetic field, it is shown that the energy per particle increases monotonically as the density increases.

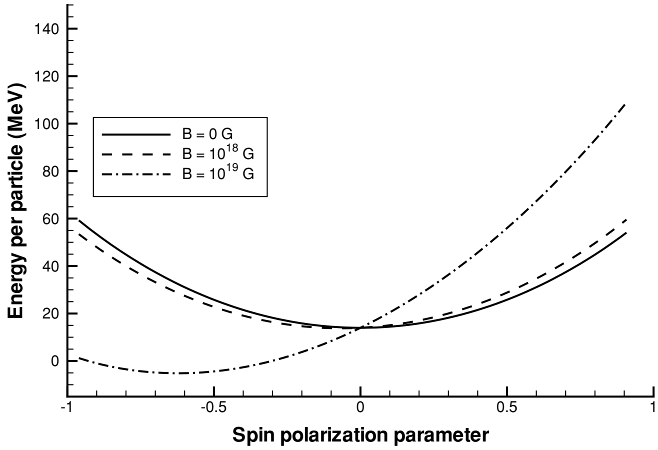

FIG. 1. The energy per particle vs the spin-polarization parameter (δ) for different values of the magnetic field (B) at $\rho = 0.2$ fm^{-3}.

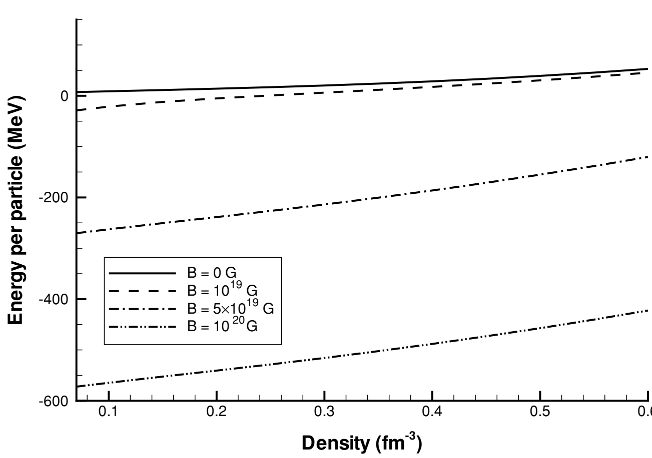

FIG. 2. The ground-state energy per particle as a function of the density at different values of the magnetic field (B).

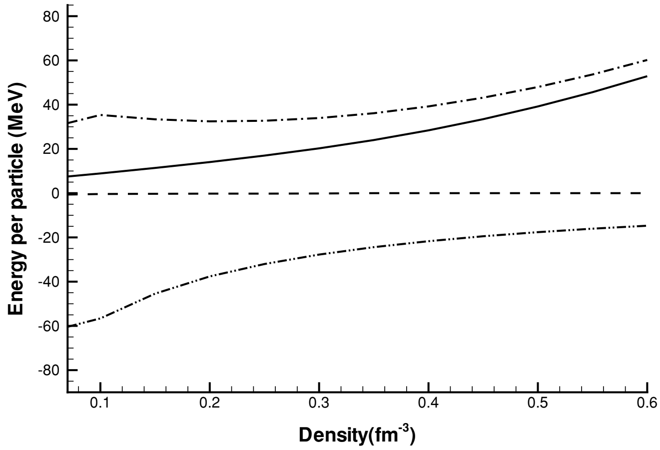

FIG. 3. The energy contribution of spin-polarized neutron matter in the cluster expansion up to the two-body term ($E_1 + E_2$) for the magnetic fields $B = 10^{18}$ G (solid curve) and $B = 10^{19}$ G (dash-dotted curve), and the contribution of magnetic energy (E_M) for magnetic fields $B = 10^{18}$ G (dashed curve) and $B = 10^{19}$ G (dash-dot-dotted curve).

However, the increasing rate of energy versus density increases when the magnetic field increases. This indicates that, at higher magnetic fields, the increasing rate of the contribution of magnetic energy versus density is more than that at lower magnetic fields. To clarify this behavior, we present the energy contribution of spin-polarized neutron matter up to the two-body term in the cluster expansion ($E_1 + E_2$), and the magnetic energy contribution (E_M) separately, as a function of density in Fig. 3. This figure shows that, for the spin-polarized neutron matter, the difference between the magnetic energy contributions (E_M) of different magnetic fields is substantially larger than that for the energy contribution ($E_1 + E_2$). Figure 4 shows the ground-state energy per particle of spin-polarized neutron matter as a function of the magnetic field for different values of density. We can see that by increasing the magnetic field up to a value of about 10^{18} G, the energy per particle slowly decreases, and then it rapidly decreases for the magnetic fields greater than this value. This indicates that, above $B \sim 10^{18}$ G, the effect of the magnetic field on the energy construction of the spin-polarized neutron matter becomes more important.

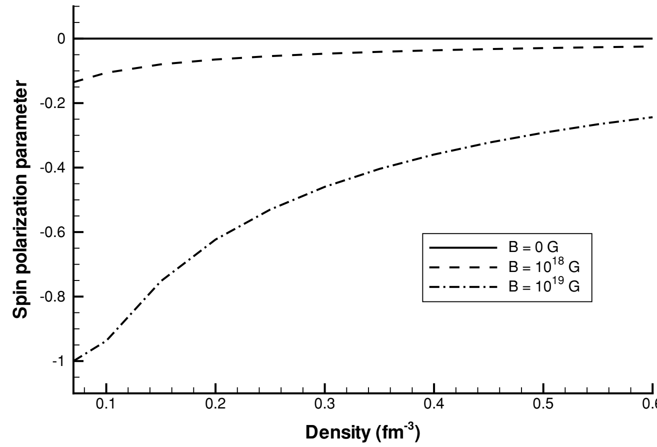

FIG. 5. The spin-polarization parameter at the equilibrium state of the system as a function of the density at different values of the magnetic field (B).

In Fig. 5, the spin-polarization parameter corresponding to the equilibrium state of the system is plotted as a function of density for different values of the magnetic field. It is seen that, at each magnetic field, the magnitude of the spin-polarization parameter decreases as the density increases. Figure 5 also shows that for the magnetic fields below 10^{18} G, at high densities, the system nearly becomes unpolarized. However, for higher magnetic fields, the system has a substantial spin polarization, even at high densities. In Fig. 6, we plot the spin-polarization parameter at equilibrium as a function of the magnetic field at different values of density. This figure shows that below $B \sim 10^{18}$ G no anomaly is observed and the neutron matter can only be partially polarized. This partial polarization is maximized at lower densities and amounts to about 14% of its maximum possible value of -1. From Fig. 6, we can also see that below $B \sim 10^{17}$ G the spin-polarization parameter is nearly zero. This clearly confirms the absence

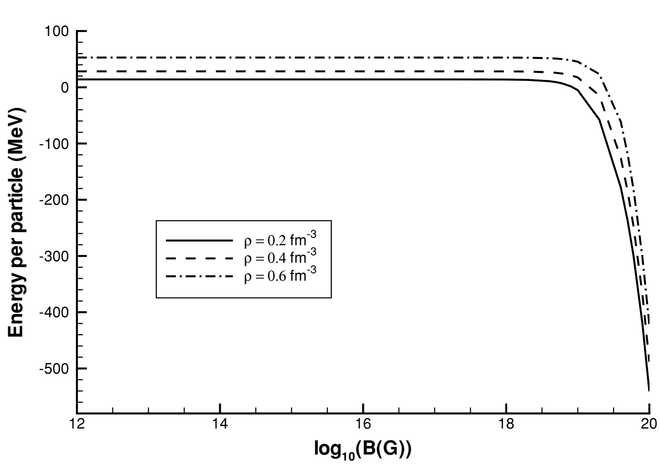

FIG. 4. The ground-state energy per particle as a function of the magnetic field (B) at different values of the density (ρ).

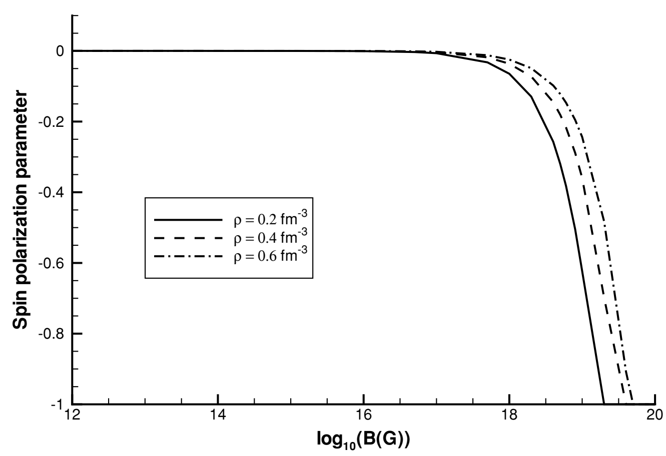

FIG. 6. The spin-polarization parameter corresponding to the equilibrium state of the system as a function of the magnetic field (B) at different values of the density (ρ).

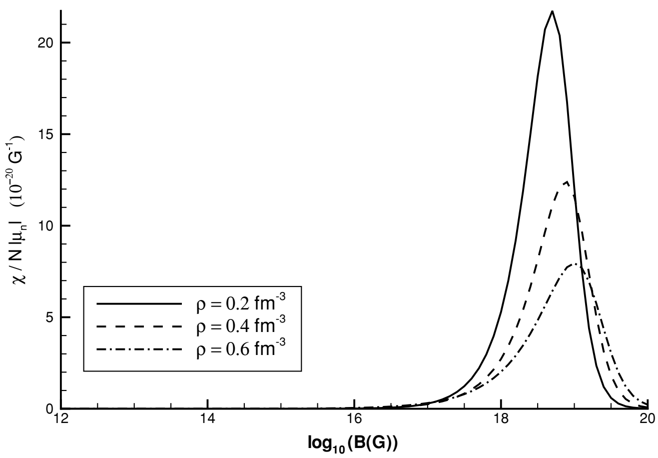

FIG. 7. The magnetic susceptibility ($\chi/N|\mu_n|$) as a function of the magnetic field (B) at different values of the density (ρ).

of magnetic ordering for neutron matter up to $B \sim 10^{17}$ G. For the magnetic fields greater than about 10^{18} G, it is shown that the magnitude of spin polarization rapidly increases as the magnetic field increases. This shows a ferromagnetic phase transition in the presence of a strong magnetic field. For each density, we can see that at high magnetic fields the value of the spin-polarization parameter is close to -1. The corresponding value of the magnetic field increases as the density increases.

The magnetic susceptibility (χ), which characterizes the response of a system to the magnetic field, is defined by

$$\chi(\rho, B) = \left(\frac{\partial M_z(\rho, B)}{\partial B}\right)_{\rho}. \quad (35)$$

In Fig. 7, we plot the ratio $\chi/N|\mu_n|$ for the spin-polarized neutron matter versus the magnetic field at three different values of the density. As can be seen from Fig. 7, for each density, this ratio shows a maximum at a specific magnetic field. This result confirms the existence of the ferromagnetic phase transition induced by the magnetic field. We see that the

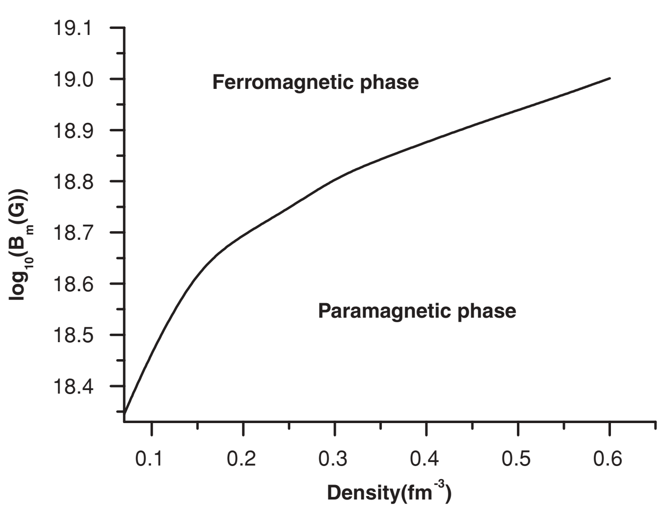

FIG. 8. Phase diagram for the spin-polarized neutron matter in the presence of a strong magnetic field.

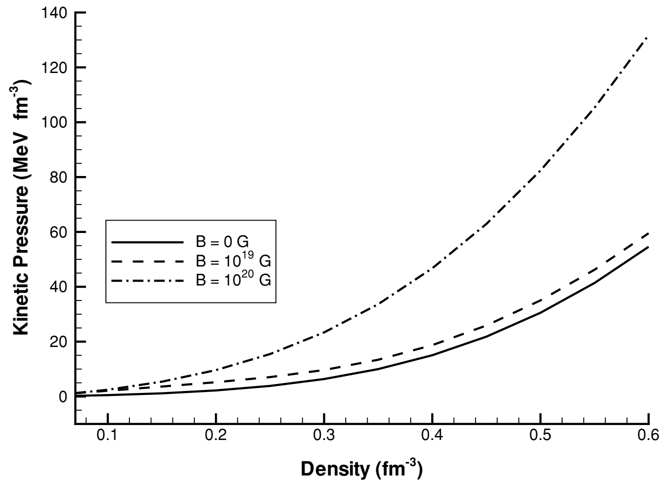

FIG. 9. The equation of state of spin-polarized neutron matter for different values of the magnetic field (B).

magnetic field at the phase transition point, B_m, depends on the density of the system. Figure 8 shows the phase diagram for the spin-polarized neutron matter. We can see that, as the density increases, B_m grows monotonically. It explicitly means that at higher densities the phase transition occurs at higher values of the magnetic field.

From the energy of spin-polarized neutron matter, at each magnetic field, we can evaluate the corresponding pressure (P_{kinetic}) using the following relation:

$$P_{\mathrm{kinetic}}(\rho, B) = \rho^2\left(\frac{\partial E(\rho, B)}{\partial \rho}\right)_{B}. \quad (36)$$

Our results for the kinetic pressure of spin-polarized neutron matter versus density for different values of the magnetic field are shown in Fig. 9. It is obvious that, as the density is increased, the difference in the pressure of spin-polarized neutron matter at different magnetic field becomes more appreciable. Figure 9 shows that the equation of state of the spin-polarized neutron matter becomes stiffer as the magnetic field strength increases. This stiffening is due to the inclusion of neutron anomalous magnetic moments. This is in agreement with the results obtained in Refs. [10,13]. It should be noted here that, to find the total pressure related for the neutron star structure, the contribution from the magnetic field, $P_{\mathrm{mag}} = \frac{B^2}{8\pi}$, should be added to the kinetic pressure [10,14]. However, in this work we are not interested in the neutron star structure and thus omit the contribution of "magnetic pressure" in our calculations for neutron matter [16]. This term, if included, simply adds a constant amount to the curves depicted in Fig. 9.

IV. SUMMARY AND CONCLUDING REMARKS

We recently calculated several properties of spin-polarized neutron matter in the absence of a magnetic field using the lowest order constrained variational method with AV_{18} potential. In this work, we generalized our calculations for spin-polarized neutron matter in the presence of a strong magnetic field at zero temperature using this method. We found that the effect of magnetic fields below $B \sim 10^{18}$ G is almost negligible. It was shown that, in the presence of magnetic field, the spin-polarization symmetry is broken and the energy per particle shows a minimum at $-1 < \delta < 0$, depending on the strength of the magnetic field. We showed that the ground-state energy per particle decreases as the magnetic field increases. This leads to a more stable system. It is seen that the increasing rate of energy versus density increases as the magnetic field increases. Our calculations show that above $B \sim 10^{18}$ G the effect of the magnetic field on the properties of neutron matter becomes more important. In the study of the spin-polarization parameter, we showed that, for a fixed magnetic field, the magnitude of the spin-polarization parameter at the minimum point of energy decreases with increasing density. At strong magnetic fields with strengths greater than 10^{18} G, our results show that a field-induced ferromagnetic phase transition occurs for the neutron matter. By investigating the magnetic susceptibility of the spin-polarized neutron matter, it is clear that, as the density increases, the phase transition occurs at higher values of the magnetic field. Through the calculation of pressure as a function of density at different values of the magnetic field, we observed the stiffening of the equation of state in the presence of the magnetic field.

Finally, we would like to address the question of the thermodynamic stability of such neutron stars at ultrahigh magnetic fields. One may wonder if the effect of magnetic pressure, $P_{\text{mag}} = \frac{B^2}{8\pi}$, which we omit here, is added to the kinetic pressure P_{kinetic}; then at ultrastrong magnetic fields, the system might become gravitationally unstable due to excessive outward pressure. For the fields considered in this work (up to 10^{20} G), this scenario does not seem likely [7]. We note that the increase of magnetic field leads to stiffening of the equation of state (Fig. 9), which in turn leads to larger mass and radius for the neutron star [40]. This in turn increases the effect of gravitational energy, offsetting the increased pressure. We also note that the existence of a well-defined thermodynamic energy minimum for all fields considered in our work indicates the thermodynamic stability of our system. The existence of such well-defined minimum energy is unaffected by the addition of magnetic energy. The detailed analysis of such situations along with the accompanying change in proton fraction is a possible avenue for future research.

ACKNOWLEDGMENTS

We would like to thank two anonymous referees for constructive criticisms. This work has been supported by the Research Institute for Astronomy and Astrophysics of Maragha. We wish to thank the Shiraz University Research Council.

[1] A. Reisenegger, Astron. Nachr. **328**, 1173 (2007).
[2] L. Woltjer, Astrophys. J. **140**, 1309 (1964).
[3] R. J. Tayler, Mon. Not. R. Astron. Soc. **161**, 365 (1973).
[4] H. Spruit, Astron. Astrophys. **381**, 923 (2002).
[5] C. Thompson and R. C. Duncan, Astrophys. J. **408**, 194 (1993).
[6] D. Lai and S. L. Shapiro, Astrophys. J. **383**, 745 (1991).
[7] S. Shapiro and S. Teukolsky, *Black Holes, White Dwarfs and Neutron Stars* (Wiley, New York, 1983).
[8] Y. F. Yuan and J. L. Zhang, Astron. Astrophys. **335**, 969 (1998).
[9] Y. F. Yuan and J. L. Zhang, Astrophys. J. **525**, 950 (1999).
[10] A. Broderick, M. Prakash, and J. M. Lattimer, Astrophys. J. **537**, 351 (2000).
[11] I. S. Suh and G. J. Mathews, Astrophys. J. **546**, 1126 (2001).
[12] W. Chen, P. Q. Zhang, and L. G. Liu, Mod. Phys. Lett. A **22**, 623 (2007).
[13] P. Yue and H. Shen, Phys. Rev. C **74**, 045807 (2006).
[14] A. Broderick, M. Prakash, and J. M. Lattimer, Phys. Lett. B **531**, 167 (2002).
[15] S. Chakrabarty, D. Bandyopadhyay, and S. Pal, Phys. Rev. Lett. **78**, 2898 (1997).
[16] A. A. Isayev and J. Yang, Phys. Rev. C **80**, 065801 (2009).
[17] A. A. Isayev and J. Yang, J. Korean Astron. Soc. **43**, 161 (2010).
[18] M. A. Perez-Garcia, Phys. Rev. C **77**, 065806 (2008).
[19] M. A. Perez-Garcia, Phys. Rev. C **80**, 045804 (2009).
[20] M. A. Perez-Garcia, J. Navarro, and A. Polls, Phys. Rev. C **80**, 025802 (2009).
[21] J. D. Anand, N. Chandrika Devi, V. K. Gupta, and S. Singh, Astrophys. J. **538**, 870 (2000).
[22] S. Ghosh and S. Chakrabarty, Pramana **60**, 901 (2002).
[23] S. Chakrabarty, Phys. Rev. D **54**, 1306 (1996).
[24] V. K. Gupta, A. Gupta, S. Singh, and J. D. Anand, Int. J. Mod. Phys. D **11**, 545 (2002).
[25] D. Bandyopadhyay, S. Chakrabarty, and S. Pal, Phys. Rev. Lett. **79**, 2176 (1997).
[26] G. H. Bordbar and A. Peyvand, Res. Astron. Astrophys. **11** (2011) (in press).
[27] C. Y. Cardall, M. Prakash, and J. M. Lattimer, Astrophys. J. **554**, 322 (2001).
[28] A. A. Isayev, Phys. Rev. C **74**, 057301 (2006).
[29] G. H. Bordbar and M. Bigdeli, Phys. Rev. C **75**, 045804 (2007).
[30] G. H. Bordbar and M. Bigdeli, Phys. Rev. C **76**, 035803 (2007).
[31] G. H. Bordbar and M. Bigdeli, Phys. Rev. C **77**, 015805 (2008).
[32] G. H. Bordbar and M. Bigdeli, Phys. Rev. C **78**, 054315 (2008).
[33] M. Bigdeli, G. H. Bordbar, and Z. Rezaei, Phys. Rev. C **80**, 034310 (2009).
[34] M. Bigdeli, G. H. Bordbar, and A. Poostforush, Phys. Rev. C **82**, 034309 (2010).
[35] J. W. Clark, Prog. Part. Nucl. Phys. **2**, 89 (1979).
[36] R. B. Wiringa, V. G. J. Stoks, and R. Schiavilla, Phys. Rev. C **51**, 38 (1995).
[37] J. C. Owen, R. F. Bishop, and J. M. Irvine, Nucl. Phys. A **277**, 45 (1977).
[38] H. B. Callen, *Thermodynamics and an Introduction to Thermostatistics* (Wiley, New York, 1985).
[39] G. H. Bordbar and M. Modarres, Phys. Rev. C **57**, 714 (1998).
[40] G. H. Bordbar and M. Hayati, Int. J. Mod. Phys. A **21**, 1555 (2006).